XAFS analysis for quantification of the gallium coordinations in Al_2O_3-supported Ga_2O_3 photocatalysts

M. Akatsuka[1], T. Yoshida[2], N. Yamamoto[1], M. Yamamoto[1], S. Ogawa[1], S. Yagi[2]
[1] Graduate School of Engineering, Nagoya University, Nagoya 464-8603, Japan
[2] Eco Topia Science Institute, Nagoya University, Nagoya464-8603, Japan

E-mail: akatsuka.masato@d.mbox.nagoya-u.ac.jp, tyoshida@ocarina.osaka-cu.ac.jp

Abstract. Ga_2O_3 loaded Al_2O_3 samples (Ga_2O_3/Al_2O_3) were prepared to change coordination structures around Ga atoms. Ga K-edge XANES spectra of the Ga_2O_3/Al_2O_3 samples showed two peaks assigned to Ga atoms having tetrahedral coordination structure (Ga(t)) and octahedral one (Ga(o)). Curve-fitting analysis of XANES spectra was carried out with a set of pseudo-Voight and arctangent functions, and the fractions of Ga(t) and Ga(o) were quantitatively estimated from the ratio of the peak areas. EXAFS curve-fitting analysis also evaluated the fractions of Ga(t) and Ga(o) and they were in good agreement with those obtained by XANES analysis. It was revealed that the fraction of Ga(t) increased with the decrease in the loading amount of Ga_2O_3 due to the interaction of Ga species with Al_2O_3. The fractions of Ga(t) and Ga(o) might relate to the photocatalytic activity for CO_2 reduction with H_2O over the Ga_2O_3/Al_2O_3 samples.

1. Introduction

Gallium oxide (Ga_2O_3) photocatalysts can reduce CO_2 to CO with H_2O, although the efficiency of CO production is very low [1]. Generally, photocatalytic activity depends on the coordination structure of the surface active site [2]. However, there are few works investigating the influence of Ga_2O_3 coordination structure on the CO_2 photoreduction activity. Ga_2O_3 has two coordination structures, tetrahedral coordination site (Ga(t)) and octahedral one (Ga(o)). In β-Ga_2O_3 crystal, for example, the ratio of Ga(t) to Ga(o) is known as 1:1 [3], and the other crystal phases of Ga_2O_3 have different ratios. In addition, it has been reported that GaAl-oxide has only Ga(t) [4]. Thus, we think that the ratio of Ga(t) to Ga(o) can be controlled by loading Ga_2O_3 on the Al_2O_3-support to improve photocatalytic activity of Ga_2O_3.

In this study, we prepared Ga_2O_3 loaded Al_2O_3 samples (Ga_2O_3/Al_2O_3) and measured Ga K-edge XAFS spectra of these samples. The fractions of Ga(t) and Ga(o) were calculated by curve-fitting analysis of XANES spectra and were confirmed by curve-fitting analysis on EXAFS of first neighboring oxygen atoms (Ga-O shell). In addition, the EXAFS of the second neighboring atoms was investigated in detail to obtain the information about interaction between Ga_2O_3 and Al_2O_3. We also carried out the photocatalytic CO_2 reduction over Ga_2O_3/Al_2O_3 samples to reveal the correlation between the photocatalytic activity and the ratio of Ga(t) to Ga(o).

2. Experiment

Ga_2O_3/Al_2O_3 samples were prepared by impregnation of γ-Al_2O_3 with aqueous solution of gallium nitrate followed by dry and calcination in the air at 773 K for 4 h, as described elsewhere [5]. The loading amounts of Ga_2O_3 were 1, 5, 10 and 20 wt%. Unsupported Ga_2O_3 sample was also prepared by calcination of gallium nitrate similarly to Ga_2O_3/Al_2O_3. The Ga_2O_3 sample was employed for XRD measurement to identify the crystal phase of Ga_2O_3. Surface areas of all the prepared samples were measured by BET method.

Content from this work may be used under the terms of the Creative Commons Attribution 3.0 licence. Any further distribution of this work must maintain attribution to the author(s) and the title of the work, journal citation and DOI.
Published under licence by IOP Publishing Ltd

The Ga K-edge XAFS measurement of the samples were conducted at the beamline 5S1 in Aichi Synchrotron Radiation Center. The beamline was equipped with Si(111) double-crystal monochromators. The data were recorded in a transmission mode or a fluorescent X-ray yield mode with a 19 channel silicon semiconductor detector.

XANES spectra were curve-fitted with pseudo-Voight function (1) and arctangent function (2).

$$f(x) = \frac{A}{[1+M(x-x_0)^2/\beta^2]\exp\{(1-M)[(ln2)(x-x_0)^2/\beta^2]\}} \quad (1)$$

$$g(x) = \mathrm{B}\left\{(1/\pi)\arctan\left(\frac{x-x_0'}{\Gamma/2}\right) + (1/2)\right\} \quad (2)$$

In these formula, A, B are heights and β, γ are full width at half maximum. x_0 and x_0' are position of the peak of pseudo-Voight curve and the inflection point of arctangent curve, respectively. M is the ratio of contribution of Lorentzian in pseudo-Voigt curve. Nishi *et al*. carried out curve-fitting with Gaussian and arctangent curves on Ga K-edge XANES spectra of Ga_2O_3 loaded Al_2O_3 samples although the Gaussian fitting arose some deviation from a XANES spectrum especially around the edge [5]. On the other hand, pseudo-Voigt curve used in this study was more suitable for the curve-fitting because XANES spectrum includes natural width due to electron excitation as well as that of the measurement system. Therefore, it is expected that the present curve-fitting leads to better accuracy in the quantitative estimation of Ga(t) and Ga(o). The fractions of Ga(t) and Ga(o) were also evaluated by the non-linear least squares curve-fitting analysis of EXAFS spectra [6].

Photocatalytic CO_2 reduction with H_2O was carried out over Ga_2O_3/Al_2O_3 and Ga_2O_3 samples. Ga_2O_3/Al_2O_3 sample was put into the fixed-bed flow reactor cell under CO_2 gas with a flow rate at 3.0 mL/min and irradiated by UV-light in the range of 254 ± 10 nm was 29.5 mW/cm^2. The reaction gases were measured with the GC-TCD (SHIMADZU, GC-8A).

3. Results and discussion

Unsupported Ga_2O_3 was identified as γ-Ga_2O_3 by the XRD pattern. On the other hand, very weak and broad lines due to Ga oxide phase were observed for Ga_2O_3/Al_2O_3 samples but could not be identified clearly. In the EDS measurements of Ga_2O_3/Al_2O_3 samples, no remarkable Ga oxide particles were observed. These results suggested that the loaded Ga_2O_3 species were highly dispersed on Al_2O_3. Based on the BET measurements for a bare Al_2O_3 and Ga_2O_3/Al_2O_3 samples, we roughly estimated the surface area of Ga oxide phase in each Ga_2O_3/Al_2O_3 sample by subtracting the component of Al_2O_3 support. We regarded that the surface areas of Ga oxide phase are almost the same each other.

Ga K-edge XANES spectra of Ga_2O_3/Al_2O_3 samples are shown in Figure 1 together with those of γ-Ga_2O_3 and β-Ga_2O_3. Two peaks shown at 10375 eV and 10379 eV are attributed to Ga(t) and Ga(o), respectively [5]. In addition, a small peak is observed around 10384 eV. This peak would be influenced by a multiple scattering of photoelectrons by neighboring atoms. The XANES spectra of the Ga_2O_3/Al_2O_3 samples showed both peaks at 10375 eV and 10379 eV, and the former peak reduced and the latter peak grew with increased amount of Ga_2O_3 supported on Al_2O_3. It is likely that the Ga_2O_3/Al_2O_3 samples contain two kinds of Ga species, Ga(t) and Ga(o), and the fraction of each species differs with the loading amount of Ga_2O_3.

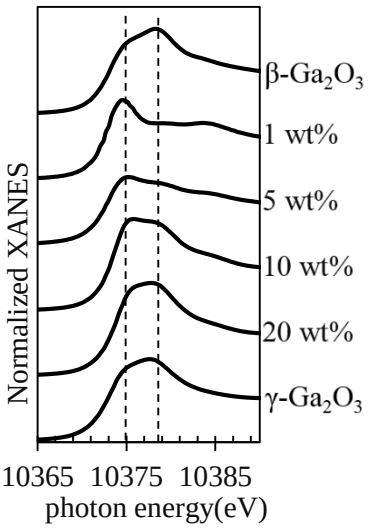

Figure 1. Ga K-edge XANES spectra of the Ga_2O_3/Al_2O_3 and Ga_2O_3 samples.

Here, we calculate the fractions of Ga(t) and Ga(o) in each Ga_2O_3/Al_2O_3 sample by curve-fitting on each XANES spectrum with two sets of pseudo-Voigt and arctangent curves. The simulation of the spectrum was made on the basis of the following assumptions: [7] 1) the spectrum is composed of two components; 2) each component consists of an arctangent curve for continuum absorption and a pseudo-Voigt curve for the white line; 3) the ratio of the height of each arctangent curve is equal to the ratio of the peak area of each pseudo-Voigt curve; 4) The small peak around 10384 eV is not employed for the curve-fitting analysis. Figure 2 shows the curve-fitting on XANES spectrum of β-Ga_2O_3. The fractions of Ga(t) and Ga(o) in β-Ga_2O_3 were evaluated as 51% and 49 %, and the fractions were well accorded with the crystal data of β-Ga_2O_3 (fractions of Ga(t) and Ga(o) are 50% and 50 %)

[8]. This result suggests that the fractions of Ga(t) and Ga(o) in Ga_2O_3/Al_2O_3 samples can be estimated quantitatively by our curve-fitting analysis, and we also decided the parameter M in the pseudo-Voigt curve as 0.7. Table 1 summarizes the other parameters used for the curve-fitting analysis on XANES spectra of Ga_2O_3/Al_2O_3 samples, and the calculated fractions of Ga(t) in the Ga_2O_3/Al_2O_3 samples are also shown in Table 2. It is revealed that the coordination structure around a Ga atom was controlled by loading Ga_2O_3 on the Al_2O_3-support and the Ga(t) was formed preferentially in the sample with lower loading amount of Ga_2O_3.

Table 1. Curve-Fitting parameters

Samples	Ga(t) species (eV)				Ga(o) species (eV)			
	position X_0	position X_0'	fwhm β	fwhm Γ	position X_0	position X_0'	fwhm β	fwhm Γ
β-Ga_2O_3	10374.9	10372	2.3	3	10378.5	10376	2.3	3
γ-Ga_2O_3	10374.3	10371.7	2	4	10378	10375	3	2.5
Ga_2O_3/Al_2O_3								
1 wt%	10374.8	10372.5	2.1	2	10379.5	10378	3	4
5 wt%	10374.6	10373	2.5	4	10378.8	10377	3.4	4
10 wt%	10375.1	10373	2.1	4	10378.6	10377	3	4
20 wt%	10375.2	10373	2.1	4	10378.5	10376	3	4

Fitting error of XANES spectrum with these parameters is ±5%.

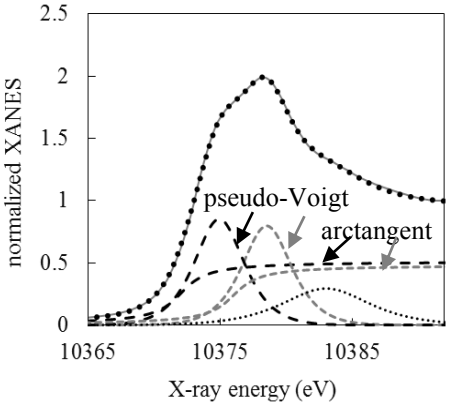

Figure 2. Ga K-edge XANES spectrum of β-Ga_2O_3 (solid line) and the simulated spectrum (dotted), which consists of two sets of pseudo-Voigt and arctangent curves (broken).

Table 2. The fraction of Ga(t) in Ga_2O_3/Al_2O_3 estimated by XANES and EXAFS analyses

sample	Loading amount of Ga_2O_3 (wt%)				
	1	5	10	20	γ-Ga_2O_3
Ga(t) (%)	75	60	46	39	36
Ga(o) (%)	25	40	54	61	64

Errors of Ga(t) and Ga(o) fractions estimated by XANES and EXAFS are ±2% and ±8%, respectively.

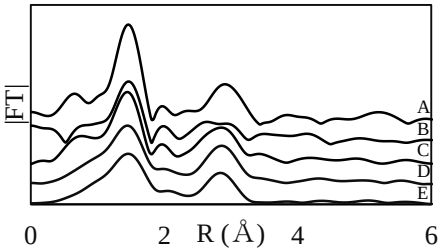

Figure 3. Radial structure functions of Ga_2O_3/Al_2O_3 and γ-Ga_2O_3. A) 1 wt% Ga_2O_3/Al_2O_3, B) 5 wt% Ga_2O_3/Al_2O_3, C) 10 wt% Ga_2O_3/Al_2O_3, D) 20 wt% Ga_2O_3/Al_2O_3, E) γ-Ga_2O_3

We also measured k^3-weighted Ga K-edge EXAFS spectra of Ga_2O_3/Al_2O_3 and γ-Ga_2O_3 samples as shown in Supporting Information with Figure S1. The Fourier transform was performed on each EXAFS spectrum in the 3-13.7 $Å^{-1}$ region and the radial structure function (RSF) was obtained as shown in Figure 3. Peak appearing at 1-2 Å is assigned to the backscattering from the adjacent oxygen atoms, and peaks around 3 Å show the presence of the second-neighboring metal atoms (Ga or Al). Note that the RSFs of the 10 and 20 wt% Ga_2O_3/Al_2O_3 samples were similar to that of γ-Ga_2O_3 rather than β-Ga_2O_3.

The first peak at 1-2 Å was sharp and high for 1 wt% Ga_2O_3/Al_2O_3 while it became broader and lower for the other Ga_2O_3/Al_2O_3 samples. We performed curve-fitting analysis for the inverse Fourier transform of the first peak at 1-2 Å with two Ga-O shells. For the reference sample, β-Ga_2O_3, the curve-fitting results indicate coordination shells with 2.0 oxygen atoms at 1.85 Å and 3.0 oxygen atoms at 2.00Å, which is in good agreement with the crystallographic data for Ga(t)-O and Ga(o)-O shells, respectively. Similar short Ga(t)-O and long Ga(o)-O shells were found for all Ga_2O_3/Al_2O_3 samples, then we estimated the fractions of Ga(t) and Ga(o) by using of the coordination numbers for Ga(t)-O and Ga(o)-O, and the results are also summarized in Table 2. The fractions of Ga(t) and Ga(o) obtained by XANES and EXAFS analyses are good agreement with each other, supporting that the fraction of Ga(t) is higher for the sample with lower loading amount of Ga_2O_3.

Here, we investigated the second-neighboring metal atoms in the low and high loaded Ga_2O_3/Al_2O_3 samples. Figure 4 shows the envelope functions of inverse Fourier transform of the second peak around 3 Å in RSFs of 1, 20 wt% Ga_2O_3/Al_2O_3 samples and γ-Ga_2O_3. The maximum in the envelope appeared at a low k value for the 1 wt% Ga_2O_3/Al_2O_3 sample while that in the other envelopes was observed at 8-9 $Å^{-1}$. This result clearly indicates that the envelope of 1wt% Ga_2O_3/Al_2O_3 sample is due to backscatterer lighter than Ga atoms, i.e., Al is very likely. Therefore, in the low loaded Ga_2O_3/Al_2O_3 sample, highly dispersed Ga species would interact with Al_2O_3 support to form Ga(t) structure, while in the high loaded

Ga_2O_3/Al_2O_3 sample, the aggregation of Ga species would produce similar structure as γ-Ga_2O_3 to decrease in the fraction of Ga(t).

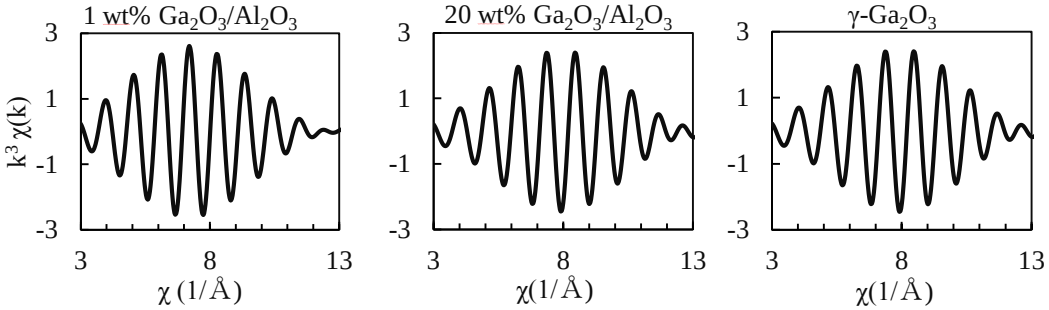

Figure 4. The envelope functions of inverse Fourier transform of the second peak around 3 Å in radial structure functions of 1, 20 wt% Ga_2O_3/Al_2O_3 and γ-Ga_2O_3.

Photocatalytic CO_2 reduction with H_2O was carried out over the Ga_2O_3/Al_2O_3 sample. CO production rates over 5, 10 and 20 wt% Ga_2O_3/Al_2O_3 samples were higher than those over β-Ga_2O_3 and Al_2O_3 samples, while over 1 wt% Ga_2O_3/Al_2O_3, it was almost the same as that over Al_2O_3 sample. At present, the reason for a small amount of CO production over 1 wt% Ga_2O_3/Al_2O_3 has not been clarified yet. This sample probably forms a GaAl-oxide and such a solid state sample might show low activity for CO_2 photoreduction.

Figure 5 shows the variation of CO production rate per a Ga atom with the fraction of Ga(t) in 5, 10 and 20 wt% Ga_2O_3/Al_2O_3 samples. As mentioned above, since Ga_2O_3 species would be highly dispersed on Al_2O_3, we assumed that the Ga(t) fraction evaluated by XANES and EXAFS corresponds to the Ga(t) fraction at the surface. In this figure, CO production rate per a Ga atom seemed to increase with the fraction of Ga(t). However, it might be required to estimate carefully the numbers of the surface Ga(t) and Ga(o) really contributing to the photocatalytic reaction by CO_2 and H_2O adsorption experiments in our future work.

4. Conclusion

Ga K-edge XAFS spectra were recorded on the Ga_2O_3 loaded Al_2O_3 photocatalysts. Curve-fitting analysis of XANES spectra could estimate the fractions of tetrahedral and octahedral Ga species (Ga(t) and Ga(o)) in these samples, which was confirmed by EXAFS curve-fitting analysis. We concluded that the fraction of Ga(t) increased with lower loading amount of Ga_2O_3. CO production rate per a Ga atom seemed to increase with the fraction of Ga(t), however, the further quantitative analysis for the surface Ga(t) and Ga(o) will be required.

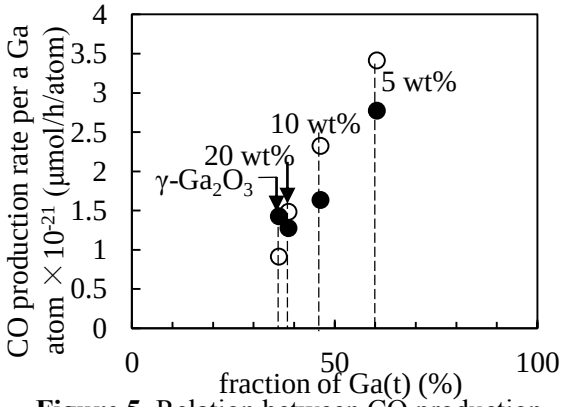

Figure 5. Relation between CO production rate per a Ga atom and the fraction of Ga(t). (○ : after 1 h, ● : after 4 h)

5. Acknowledgment

This work was supported by a Grant-in-Aid for Scientific Research (No.24360332 and 24656489) from the Japan Society for the Promotion of Science (JSPS). Synchrotron experiments were carried out at Aichi Synchrotron Radiation Center which is supported by No.201505044.

References

[1] Yoshida H, Zhang L, Sato M, Morikawa T, Kajino T *et al*. 2015 *Catal. Today* **251** 132.
[2] Yoshida S *et al*. 1992 *Catal. Lett.* **12** 277.
[3] Cramer S *et al*. 1976 *J. Am. Chem. Soc.* **98** 1287.
[4] Takahashi M *et al*. 2005 *SPring-8 User Experiment Report* **No. 15 A** 261.
[5] Nishi K, Shimizu K, Takamatsu M, Yoshida H *et al*. 1998 *J. Phys. Chem.* B **102** 10190.
[6] Yoshida T, Tanaka T, Yoshida H, Funabiki T and Yoshida S 1996 *J. Phys. Chem.* **100** 2302.
[7] Kato Y *et al.* 2001 *Phys. Chem. Chem. Phys.* **3** 1925
[8] Geller S 1960 *J. Chem. Phys.* **33** 676.